ACS APPLIED BIO MATERIALS

www.acsabm.org

Article

Easy Fabrication of a Polymeric Transparent Sheet to Combat Microbial Infection

Brinta Bhattacharjee, Sudip Mukherjee, Riya Mukherjee, and Jayanta Haldar*

Cite This: ACS Appl. Bio Mater. 2022, 5, 3951−3959

Read Online

ACCESS | Metrics & More | Article Recommendations | Supporting Information

ABSTRACT: Surges in infectious diseases and their transmission in households and commercial and healthcare settings have increased the use of polymeric materials as protective covers. Despite ongoing efforts, conventional polymeric materials still pose the threat of surface-associated transmission of pathogens due to the fact that they lack antimicrobial properties. Here, we have developed an easy-to-fabricate polymeric sheet [quaternary polymeric transparent sheet (QPTS)] that shows an excellent antimicrobial property and is also transparent in nature, increasing its practical applications in a wide range of surfaces. The sheet was fabricated by combining cationic amphiphilic water-soluble polyethylenimine derivative (QPEINH-C_6) and poly(vinyl alcohol) (PVA). The optimum composition (QPTS-3) exhibited a complete reduction of bacterial and fungal infection (∼3−4 log reduction) within 15 min. QPTS-3 also exhibited activity against antibiotic-insusceptible metabolically inactive bacterial cells. The sheet prevented the growth of MRSA biofilm even after 72 h of incubation, which was confirmed through electron microscopy on the QPTS sheet. Most importantly, ∼99.9% of the influenza viral load was reduced completely within 30 min of exposure of the sheet. Apart from the antimicrobial property, the sheet successfully retained its transparency (∼88%) and maintained a significant mechanical strength (∼15 N), highlighting its potential applications in commercial and healthcare settings.

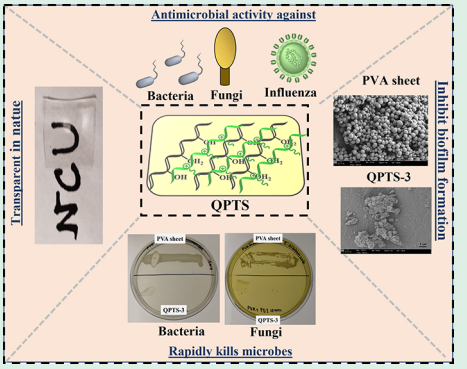

KEYWORDS: *transparent, antimicrobial film, antiviral, antifungal, antibacterial*

1. INTRODUCTION

Pathogens encompassing bacteria, fungi, and viruses have posed an enormous threat to mankind.[1] The world continues to witness unprecedented deaths and challenges due to the ongoing pandemic.[2−4] Such pathogens can colonize onto different surfaces and form fomites that contribute to nearly 50% of infection-spread in human beings.[5,6] The survival time of pathogens on surfaces is further prolonged due to their capacity to form biofilms that significantly retard the eradication process. The emergence of drug-resistance in pathogens has further exacerbated the situation, increasing mortality in clinical settings. Therefore, there is always a need for alternative antimicrobial strategies.[7−12]

Human-to-human transmission of pathogens is increased many-fold by various human actions like coughing, sneezing, talking, and breathing. Aerosolized droplets with the pathogenic load can transmit through mucosal openings such as the mouth, nose or deposit onto daily-use inanimate surfaces such as doorknobs, tables, electronic gadgets, food packets, and keypads of money-withdrawal machines. These contaminated surfaces, once touched by a healthy individual, can lead to the spread of notorious infections. Despite regular sterilization in hospital settings, offices, or in regular households, the infection-spread has remained a persistent concern.[13−15] In recent time, plastic sheets are widely used as a protective barrier in public places to reduce the chance of infection spread. Despite these efforts, the polymeric covers often fail as they are devoid of antimicrobial properties. Therefore, developments of protective polymeric covers that have antimicrobial properties are highly needed to prevent surface-mediated infection spread and accumulation of pathogens on surfaces.[16,17] It is also required for the antimicrobial polymeric covers to be transparent for their broader applicability.

Toward these goals, here, we report an easy-to-fabricate polymeric sheet [quaternary polymeric transparent sheet (QPTS)] that satisfies both the criteria of having an excellent antimicrobial property and transparency for applications in a broad range of commonly used surfaces. A modified polyethylenimine-based water-soluble cationic amphiphilic polymer was combined with a poly(vinyl alcohol) (PVA) matrix to fabricate the transparent sheet. The surface of the fabricated material was characterized using various microscopic

Received: May 21, 2022
Revised: July 3, 2022
Accepted: July 5, 2022
Published: July 31, 2022

https://doi.org/10.1021/acsabm.2c00476
ACS Appl. Bio Mater. 2022, 5, 3951−3959

and spectroscopic techniques along with an investigation of their mechanical properties. The transparent nature of the sheet was also examined using UV−vis spectroscopy. The bactericidal activity of the sheet (QPTS-3) was tested against planktonic and stationary phase bacteria. Inhibition of the biofilm formation on the sheet and its antifungal property were further examined to confirm the antimicrobial property. The transparent sheet was also exposed to influenza viruses to examine its antiviral efficacy. It is anticipated that the developed PVA-based antimicrobial sheet (QPTS) being an optically transparent sheet would encourage its widespread use in household, offices, banks, and hospitals to stop the direct spread or that it can also be employed as a cover on objects such as laptops, computer keyboards, calculators, or any other surfaces that are highly susceptible to microbial contamination.

2. MATERIALS AND METHODS

2.1. Materials and Instruments. Poly(vinyl alcohol) (40 kDa) was purchased from Sigma-Aldrich. HIMEDIA supplied bacterial and fungal growth media and agar . Fungal strains (*Candida albicans* AB226 and *C. albicans* AB399) were supplied by Anthem Biosciences, Bangalore, India. Influenza (A/NWS/33) was purchased from ATCC (Rockville, MD). Bacterial strains *Escherichia coli* MTCC 443, *Pseudomonas aeruginosa* MTCC 424, and *Acinetobacter baumannii* (MTCC 1425) were purchased from MTCC (Chandigarh, India). Bacterial strains methicillin-resistant *Staphylococcus aureus* (MRSA ATCC 33591) and *Klebsiella pneumoniae* (ATCC 700603) were obtained from ATCC (Rockville, MD). *P. aeruginosa* R590 , *A. baumannii* R674, *and E. coli* R3336 were obtained from NIMHANS (National Institute of Mental Health and Neurosciences), Bangalore, India. VRSA 1, VRSA 4, and VRSA 12 were obtained from Central Drug Research Institute (CDRI). A TECAN (Infinite series, M200) plate reader was used to record optical density (OD). Nutrient agar for bacteria and YPD agar for fungi as a solid media were used for experiments. 24-well, 12-well, and 6-well plates were purchased from Vasa Scientific, Bangalore, India.

2.2. Synthesis and Characterization of Quaternary Polyethylenimine Derivative (QPEINH-C_6). Synthesis and characterization of QPEINH-C_6 are detailed in the Supporting Information following the published protocol.[18]

2.3. Preparation of the Transparent Polymeric Sheet. *2.3.1. Fabrication of the PVA Sheet.* For the preparation of the control sheet (PVA sheet), 3 mL of poly(vinyl alcohol) (PVA, 200 mg/mL) solution (dissolved at 90 °C in water) was mixed with 1 mL of a water and DMSO mixture (1:1) to obtain a 15 wt % PVA solution. The whole solution was cast onto a 9 × 4 cm^2 plastic container and evaporated for 12 h at 60 °C to obtain the sheet.

2.3.2. Fabrication of Antimicrobial Transparent Sheets. Antimicrobial sheets (QPTSs) and a PVA sheet were fabricated to determine which is optimum. 3 mL of poly(vinyl alcohol) (PVA, 200 mg/mL) solution (dissolved at 90 °C in water) was mixed with 1 mL of QPEINH-C_6 solution (200 mg/mL, 80 mg/mL, 40 mg/mL, and 8 g/mL, dissolved in a 1:1 DMSO and water mixture). The final concentration of PVA was maintained at 15 wt %. The whole solution was cast onto a 9 × 4 cm^2 plastic container and evaporated for 12 h at 60 °C to obtain the sheet. Thus, final concentrations of the polyethylenimine based polymer (QPEINH-C_6) in QPTS-1, QPTS-2, QPTS-3, and QPTS-4 sheets were 5, 2, 1, and 0.2 wt %, respectively.

2.4. Characterization of Sheets. *2.4.1. Tensile Strength of Sheets.* Mechanical properties of polymeric sheets (PVA sheet, QPTS-1, QPTS-2, QPTS-3, and QPTS-4) were measured in a dynamic mechanical analyzer (DMA, TA Instruments). The sheets were cut to dimensions of 5 × 1.5 × 0.02 cm^3 and fixed in between the tension clamps of the DMA instrument. After loading the samples, tensile strength testing was performed using tensile force (extensional strain) at a speed of 200 μm/s up to its breaking point. The maximum force required to tear the sheets apart was considered as tensile strength. The variation of the forces was recorded with the varied strain percentage.

2.4.2. Notch Test for the QPTS-3 Sheet. The transparent sheet QPTS-3 also underwent the notch test. A sheet of dimensions 5 × 1.5 × 0.02 cm^3 was loaded in between the tensile clamp without defects and with a 5 mm linear defect. After loading the samples, tensile strength testing was performed at a speed of 200 μm/s up to its breaking point.

2.4.3. Transparency Measurement of Transparent Sheets. The PVA sheet and QPTS-3 sheet (1 × 1 cm^2) were placed in a 24-well plate, and the absorbance was measured in the visible range (400−700 nm) to determine the percentage of transmittance (%T) of the material using the following equations. The absorbance of the blank well plate (A_b) was also measured and subtracted from the absorbance of the sheet (A) to obtain the actual absorbance (A_s) of the sheet.

$$A_s = A - A_b$$

$$\%T = \text{antilog}(2 - A_s)$$

2.4.4. Swelling Property of Sheets. Preweighed 1 × 1 cm^2 sheets (PVA sheet and QPTS-3) were immersed in 1 mL of distilled water in a 2 mL centrifuge tube. Each one day interval, the sheet was taken out and gently wiped with tissue paper to remove the unsoaked water. Afterward, the weight of the sheets was measured to determine the swelling ratio. The swelling ratios of the sheets were measured for up to 3 days.

$$\text{swelling ratio (SR)} = (W_1 - W_0)/W_0$$

Here, W_1 is the weight of the swelled sheet measured after removing the excess unabsorbed water, and W_0 is the weight of the dry sheet.

2.5. Antibacterial Activity Testing through Visual Turbidity Method. A single colony of bacteria was grown for 6 h in nutrient broth to obtain the liquid culture of planktonic bacteria. A PVA sheet and QPTS-3 sheet (1 × 1 cm^2) were placed into the 12-well plate and challenged with 20 μL of bacterial suspension in saline (MRSA ATCC 33591, ∼10^6 CFU/mL). These bacterial-solution-containing sheets were incubated for different time intervals (1, 4, and 6 h). Different replicates of sheets were utilized for different time intervals. After each incubation period, the sheets were transferred to fresh MHB (Mueller−Hinton broth media) in the Falcon plate and kept under shaking conditions for 18 h to verify bacterial growth through visual turbidity. After that, 10 μL from the Falcon plate was drop-cast on the nutrient agar plate to verify the bacterial growth.

2.6. Antibacterial Activity of Transparent Sheet after Washing. The polymeric sheet QPTS-3 (dimension of 4 × 4 cm^2) was cut and placed on a plain surface and cleaned with alcohol−water-based surface cleaning spray. Every time, the cleaning agent was sprayed and then wiped with a tissue. This process was continued 50 times. After that, a small portion (1 × 1 cm^2) was cut from the sheet and used for further antibacterial testing. The sheet was challenged with 20 μL of bacterial (MRSA ATCC 33591, ∼10^6 CFU/mL) suspension in saline and incubated for 1 h. After 1 h, the sheet was transferred to fresh MHB media to incubate for 18 h to verify bacterial growth through visual turbidity. The following day, 10 μL was drop-cast onto the agar plate to verify the bacterial presence.

2.7. Antibacterial Activity of Sheets against Planktonic Phase Bacteria through the Drag Method. A PVA sheet and QPTS-3 sheet (1 × 1 cm^2) were placed in a 12-well plate. Mid log phase bacteria (MRSA ATCC 33591, *E. coli* MTCC 443, *E. coli* R3336, *A. baumannii* MTCC 1425, *A. baumannii* R674, *P. aeruginosa* ATCC 424, *K. pneumoniae* ATCC 700603, and *P. aeruginosa* R590) grown in nutrient broth at 37 °C for 6 h (about 10^8 CFU/mL) were diluted in saline to ∼10^6 CFU/mL. 20 μL of bacteria (10^6 CFU/mL in saline) was added onto the sheets and incubated at 37 °C for 1 h. After 1 h, the sheets were dragged onto the agar plate and incubated for 24 h at 37 °C to verify the bacterial growth. Images of the plates were captured for future representations.

2.8. Antibacterial Activity of Sheets against Stationary Phase Bacteria. 5 μL of a liquid culture of planktonic bacteria was

https://doi.org/10.1021/acsabm.2c00476
ACS Appl. Bio Mater. 2022, 5, 3951−3959

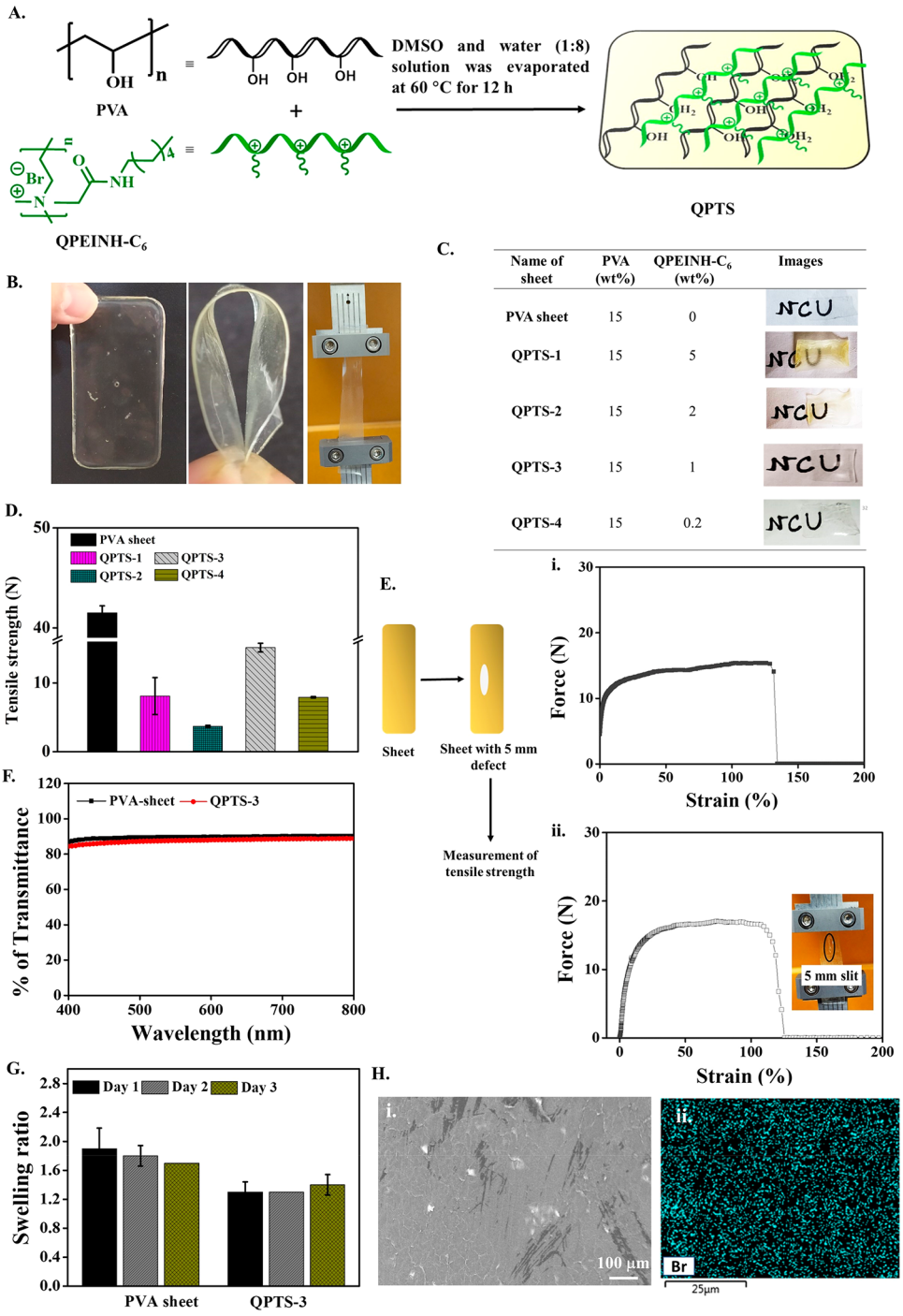

Figure 1. (A) Preparation of antimicrobial transparent sheets (QPTSs). (B) Representative photographic images of the QPTS-3 sheet. (C) Composition and photographic images of the control sheet (PVA sheet) and antimicrobial transparent sheets (QPTSs). (D) Mechanical strength of polymeric sheets (QPTSs). (E) Mechanical strength of the QPTS-3 sheet during the notch test: (i) tensile strength of the QPTS-3 sheet without defects and (ii) tensile strength of the QPTS-3 sheet with a defect. (F) Transparency measurement of polymeric transparent sheets (PVA sheet and QPTS-3) through UV−vis spectroscopy. (G) Swelling property of polymeric sheets (PVA sheet and QPTS-3). (H) (i) Visualization of the surface morphology of QPTS-3 through FESEM. Scale bar 100 μm. (ii) Elemental mapping of bromine in the QPTS-3 sheet. Scale bar 25 μm.

incubated in 5 mL of nutrient broth for 16 h to obtain stationary bacteria cells. 1 × 1 cm^2 sheets (PVA sheet and QPTS-3) were placed in a 12-well plate. Stationary phase bacteria cells (MRSA ATCC 33591, *E. coli* MTCC 443, *E. coli* R3336, *A. baumannii* MTCC 1425, *A. baumannii* R674, *P. aeruginosa* ATCC 424, *P. aeruginosa* R590, and *K. pneumoniae* MTCC 700603, about 10^8 CFU/mL) were diluted in saline to ~10^5−10^6 CFU/mL. 20 μL of stationary bacteria cells (10^5−10^6 CFU/mL in saline) was added onto the sheet and incubated at 37 °C for 1 h. After 1 h, the sheets were dragged onto the agar plate and incubated for 24 h at 37 °C to verify the bacterial growth. Images of the plates were captured for future representations.

2.9. Time Kill Kinetics of Transparent Sheets. *2.9.1. Bactericidal Kinetics of Transparent Sheets.* Replicates of 1 × 1 cm^2 sheets (PVA sheet and QPTS-3) were placed in a 12-well plate for each time point to perform the kinetics. For bacteria (MRSA ATCC 33591, *P. aeruginosa* R590, and *K. pneumoniae* ATCC 700603), both mid log phase and stationary phase cultures were diluted in saline to obtain ~10^6 CFU/mL solution. 20 μL of bacteria (10^6 CFU/mL in saline)

https://doi.org/10.1021/acsabm.2c00476
ACS Appl. Bio Mater. 2022, 5, 3951−3959

solution was added on top of the sheets and incubated at 37 °C for different time points. After incubation for the desired time intervals (0, 15, and 30 min), the sheets were dragged onto the nutrient agar plates. The agar plates were incubated for 24 h at 37 °C to detect bacterial growth. The following day, the agar plates were imaged.

2.9.2. Fungicidal Kinetics of Transparent Sheets. A single fungal colony was incubated in YPD (yeast extract−peptone−dextrose) media for 10 h to grow a fungal liquid culture (about 10^8 CFU/mL). 20 μL of a fungal solution of *C. albicans* strains (*C. albicans* AB226 and *C. albicans* AB399, 10^6 CFU/mL, diluted in saline) was exposed to 1 × 1 cm^2 sheets (PVA sheet and QPTS-3) and incubated for different time points (0, 15, and 30 min) After each time point, sheets were dragged onto YPD agar plates to verify the fungal growth.

2.10. Inhibition of Biofilm Growth on Transparent Sheets. Replicates of 1 × 1 cm^2 sheets (PVA sheet and QPTS-3) were placed in a 12-well plate. After that, 2 mL of a mid log phase MRSA ATCC 33591 bacterial suspension in biofilm media [~10^5 CFU/mL suspended in nutrient broth supplemented with 1% (w/v) NaCl and 1% (w/v) glucose] was added to the wells containing sheets and incubated for different time points (24, 48, and 72 h) to verify the bacterial growth. For individual time intervals, different replicates have been used in this experiment. After each interval (24, 48, and 72 h), the sheets were placed in another 6-well plate, and then, 1 mL of trypsin-EDTA + saline (1:9, v/v) solution was used in each plate to detach the biofilm. The biofilms were scratched and collected. Solution was diluted serially and plated on agar to count the viable bacterial burden in biofilms.

One set of sheets (PVA sheet and QPTS-3) from this experiment was processed for FESEM imaging. The PVA sheet and QPTS-3 sheets, both incubated with bacteria cells (suspended in biofilm media), were washed gently with saline and the adhered cells fixed using 2.5% (v/v) glutaraldehyde. After that, sheets were dehydrated serially using 30%, 50%, 70%, 90%, and 100% (v/v) ethanol solution and were dried. Finally, the sheets were gold sputtered, and FESEM images were captured to verify the viable bacterial presence in the biofilms.

2.11. Antiviral Assay of Sheets against the Influenza Virus. To evaluate the antiviral activity of sheets (PVA sheet and QPTS-3), a plaque assay was performed following a previous report.[19] Initially, 1 × 1 cm^2 sheets (PVA sheet and QPTS-3) were placed in a 30 mm Petri dish. A 10 μL droplet of a PBS-buffered solution of viruses [~8 × 10^5 PFU/mL for A/NWS/33 (H1N1)] was exposed onto the sheet surface for 30 min. Then, 990 μL of PBS was used to thoroughly wash the sheets, and supernatant solutions with virus particles were collected. After that, the solution was diluted and infected to a monolayer of Madin−Darby canine kidney (MDCK) cells. In the case of the QPTS-3 sheet, the collected supernatant without any dilution and its 2-fold serially diluted solutions are utilized to perform a plaque assay. In the case of the PVA sheet, the collected supernatant with viral particles was diluted 100 times, and after that, the 100× diluted solution was further serially diluted two-fold. For this serially diluted solutions with viral particles, a plaque assay was performed. In the case of the plaque assay, MDCK cells were initially seeded in a 6-well plate at 37 °C in a humidified-air atmosphere (5% CO_2/95% air) until the cells reached ~95% confluency with ~5 × 10^6 cells per well. 2 mL of DMEM cell culture media (supplemented 10 % FBS along with 1% anti-anti) was added to the 6-well plate that, which was supplied during the cell culture. The medium was removed, and MDCK cells were washed with PBS. MDCK cells were infected with solutions (200 μL) containing viral particles. At room temperature, the plates were incubated for 1 h. Rocking was performed frequently to avoid the drying of the plate. Then, the solutions were removed, and 2 mL of plaque medium with Oxoid agar (2 wt %) was poured on top of the cell layer followed by incubation at 37 °C for 72 h.

3. RESULTS AND DISCUSSION

3.1. Preparation and Characterization of Transparent Sheets (QPTSs). An antimicrobial polymeric sheet was prepared by mixing the aqueous solutions of quaternary polyethylenimine derivative (QPEINH-C_6) (synthesis is provided in the Supporting Information, Figure S1) and biocompatible polymer poly(vinyl alcohol) (PVA). The polymeric solution was dried at heating conditions (60 °C) to obtain the quaternary polymeric sheets (QPTSs) (Figure 1A). It was hypothesized based on previous reports that amide bonds in the antimicrobial polymer may interact with hydroxyl groups of poly(vinyl alcohol) through the formation of hydrogen bonds, thereby giving rise to a polymeric sheet.[20−22] Flexibility of the sheet was observed by manually stretching and bending a piece of the QPTS sheet (Figure 1B). To obtain transparency in the developed antimicrobial sheet (QPTS), the weight percentage of the cationic amphiphilic polyethylenimine derivative (QPEINH-C_6) was varied from 5 to 0.2 wt %. Four compositions, namely, QPTS-1, QPTS-2, QPTS-3, and QPTS-4 with 5, 2, 1, and 0.2 wt % of the polyethylenimine derivative, respectively, were made. Only the PVA sheet was prepared to be used as a control. In the case of all four compositions of polymeric sheets (QPTSs) and the control sheet (PVA sheet), the weight percentage of the poly(vinyl alcohol) was maintained at 15 wt %. At a higher loading percentage of the quaternary compound in QPTS sheets (QPTS-1 and QPTS-2), transparency was not achieved after solvent evaporation, and both sheets appeared to be significantly yellowish in nature. In the cases of QPTS-3 (1 wt %) and QPTS-4 (0.2 wt %), the transparency was retained even after QPEINH-C_6 incorporation (Figure 1C). Further, the prepared sheets (PVA sheet, QPTS-1, QPTS-2, QPTS-3, and QPTS-4) were tested for their mechanical property and stability by examining the maximum strength required to tear them (tensile strength). While the PVA sheet exhibited a tensile strength of ~40 ± 0.7 N, the QPTS sheets showed a tensile strength in the range ~3.7−15 N (~8 ± 2 N for QPTS-1, ~3.7 ± 0.1 N for QPTS-2, ~15 ± 0.6 N for QPTS-3, and ~7.9 ± 0.1 N for QPTS-4) (Figure 1D). The reduction of the tensile strength of the QPTS sheets may be due to reduced interactions of the PVA chains in the sheet upon addition of the cationic polymer (QPEINH-C_6). QPTS sheets did not show any trend in tensile strength; sheets containing a higher wt % of QPEINH-C_6 [5 wt % (QPTS-1) and 2 wt % (QPTS-2)] exhibited nontransparency due to uneven blending and a decrement in solubility of QPEINH-C_6 during solvent evaporation in the preparation step. However, at a lower concentration in the cases of QPTS-3 (1 wt % of QPEINH-C_6) and QPTS-4 (0.2 wt % of QPEINH-C_6), both the samples produced transparent sheets, as the blending of QPEINH-C_6 was homogeneous. QPTS-3 showed a higher tensile strength (15 N) as compared to QPTS-4 (7.9 N), which might be due to favorable interactions through hydrogen bonding and hydrophobic interaction due to the presence of amide groups and lipophilic moieties in QPEINH-C_6.

Keeping in mind the optical transparency and the mechanical stability factor, the QPTS-3 sheet was used further as it attained a better visual transparency and tensile strength as compared to the other QPTS sheets. For further evaluation, QPTS-3 with a 5 mm defect was subjected to tensile testing to detect the impact of defects on its material property. From this notch test, it is evident that, with and without defects, both cases required ~15 N of force to break the sheet completely (Figure 1E). Overall, the transparent sheet was found to possess significant mechanical properties and retain them even under a defected condition. When the transmittance was measured at the visible range (400−700 nm) using UV−vis

https://doi.org/10.1021/acsabm.2c00476
ACS Appl. Bio Mater. 2022, 5, 3951−3959

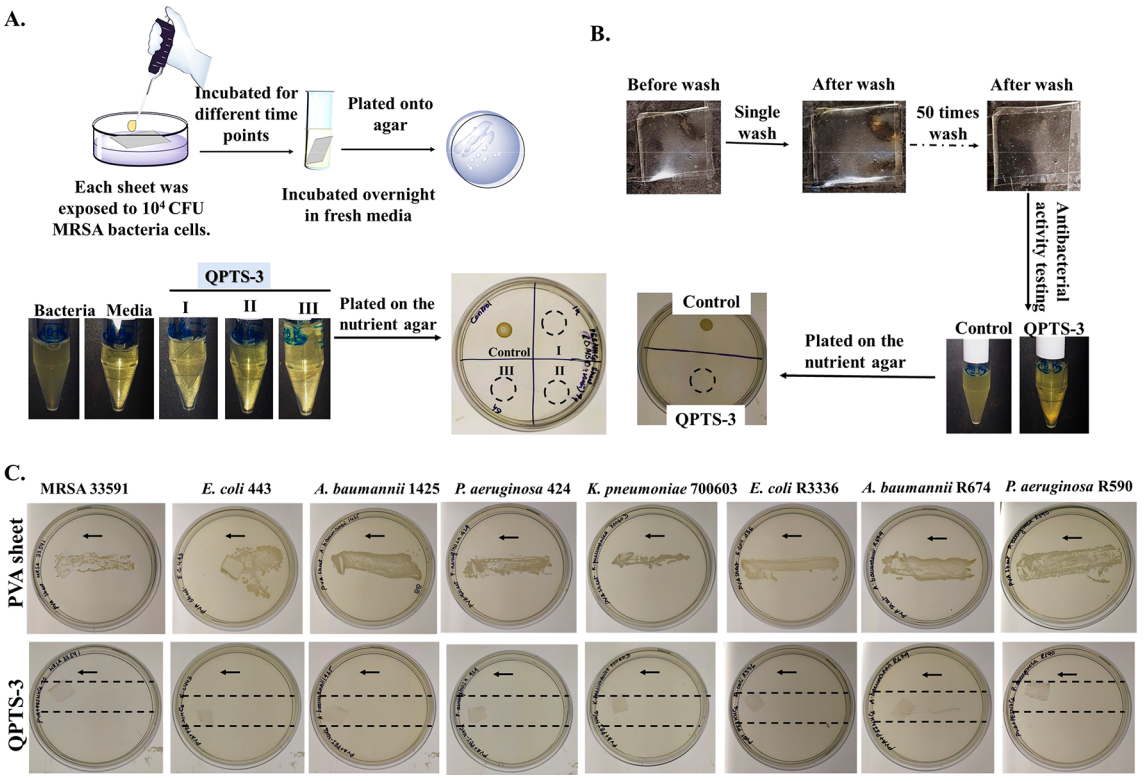

Figure 2. (A) Antibacterial activity of a polymeric transparent sheet (QPTS-3) against MRSA ATCC 33591 bacteria cells through the visual turbidity method after incubation for different time points. Experiment I, incubation time 1 h; experiment II, incubation time 4 h; and experiment III, incubation time 6 h. (B) Antibacterial activity of QPTS-3 against MRSA cells after washing with surface cleaner (water−alcohol based). (C) Antibacterial activity of a control sheet (PVA sheet) and polymeric transparent sheet (QPTS-3) against planktonic cells of bacteria. The arrow indicates the direction of dragging of the sheet on the agar plate. The dotted circle indicates an absence of bacterial growth on the agar. Dotted lines indicate the path of dragging.

spectroscopy, the PVA sheet exhibited 86−90% transmittance. On the other hand, 84−88% transmittance was obtained for the QPTS-3 sheet. This transmittance data suggests that the incorporation of antimicrobial polymer QPEINH-C_6 into PVA did not have a significant effect on the transparency of the material (Figure 1F). The PVA sheet and QPTS-3 were also dipped into water to observe the swelling property, as often, the industrial use of materials is restricted because of their water absorption tendency with a high aqueous swelling ratio. The PVA sheet absorbed water 1.9 ± 0.3 at day 1, 1.8 ± 0.1 at day 2, and 1.7 at day 3. Therefore, the swelling ratio of the PVA sheet was monitored for up to 3 days, and it absorbed water at ∼1.7−1.9 times its initial dried weight. However, QPTS-3 absorbed water 1.3 ± 0.1 at day 1, 1.3 at day 2, and 1.4 ± 0.1 at day 3. Therefore, the QPTS-3 sheet showed a water absorption of only ∼1.3−1.4 times its initial weight. This water absorption data implied that blending of the QPEINH-C_6 slightly decreased the swelling ratio of the sheet, enhancing its potential for industrial applications (Figure 1G). To understand the surface morphology of the sheets, the surface of QPTS-3 was imaged through FESEM which depicted a smooth and uniform surface texture (Figure 1H,i). The presence of bromine in the FESEM elemental mapping ascertained the uniform incorporation of the antimicrobial component of QPEINH-C_6 in the sheet (Figure 1H,ii). A thermogravimetric analysis (TGA) of the QPTS-3 sheet exhibited a 13% weight loss in the ∼85−250 °C range and ∼31% weight loss in the ∼250−330 °C range. The thermal stability of the QPTS-3 sheet was observed up to ∼85 °C (Figure S2). The glass transition temperatures (T_g) were determined using differential scanning calorimetry (DSC), and it was found to be 74 °C for the PVA sheet and 70 °C for the QPTS-3 sheet (Figure S3).

3.2. Antibacterial Activity of a Polymeric Transparent Sheet through the Visual Turbidity Method. The transparent sheet QPTS-3 was further evaluated for antibacterial activity against drug-resistant superbug MRSA ATCC 33591. Almost 10^4 CFU bacteria cells were exposed to the QPTS-3 sheet for different time points (1, 4, and 6 h). After that, bacterium incubated sheets were transferred to fresh media and incubated further to observe any residual bacterial growth. Finally, the contaminated-sheet-immersed solutions were also plated on agar for each sample. An absence of visual turbidity and no growth of bacterial colonies on the agar were observed at all of the tested time points (1, 4, and 6 h) for the QPTS-3 sheet. However, a bacterial lawn was observed in the untreated bacteria control case. An absence of visual turbidity and bacterial colonies after plating confirms that the sheet rapidly reduced the bacterial burden within 1 h (Figure 2A).

Sheets developed through this work are expected to be used repetitively for longer periods and shall be subjected to be cleaned in households or healthcare settings. Henceforth, this necessitated a reassessment of the bactericidal effectivity after repeated cleaning of the sheets. After repeated cleaning for 50 cleaning cycles with a household alcohol-based surface cleaner, a 1 × 1 cm^2 QPTS-3 sheet was again exposed to ∼10^4 CFU MRSA bacteria cells for 1 h. When assessed through the visual

https://doi.org/10.1021/acsabm.2c00476
ACS Appl. Bio Mater. 2022, 5, 3951−3959

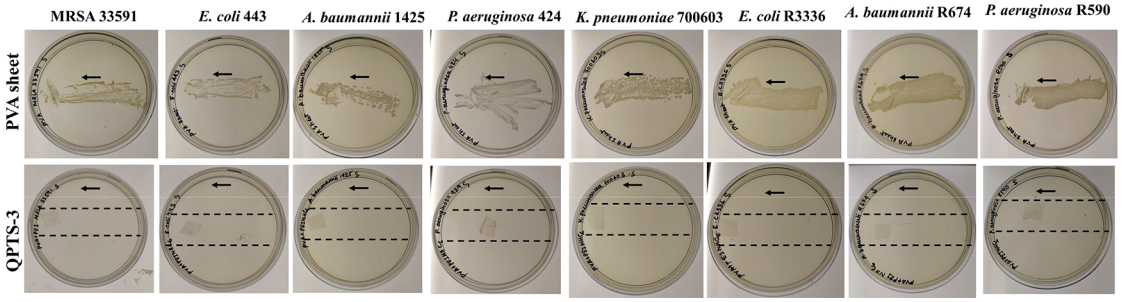

Figure 3. Antibacterial activity of the PVA sheet and QPTS-3 against stationary cells of bacteria. The arrow indicates the direction of dragging of the sheet on the agar plate. Dotted lines indicate the path of dragging.

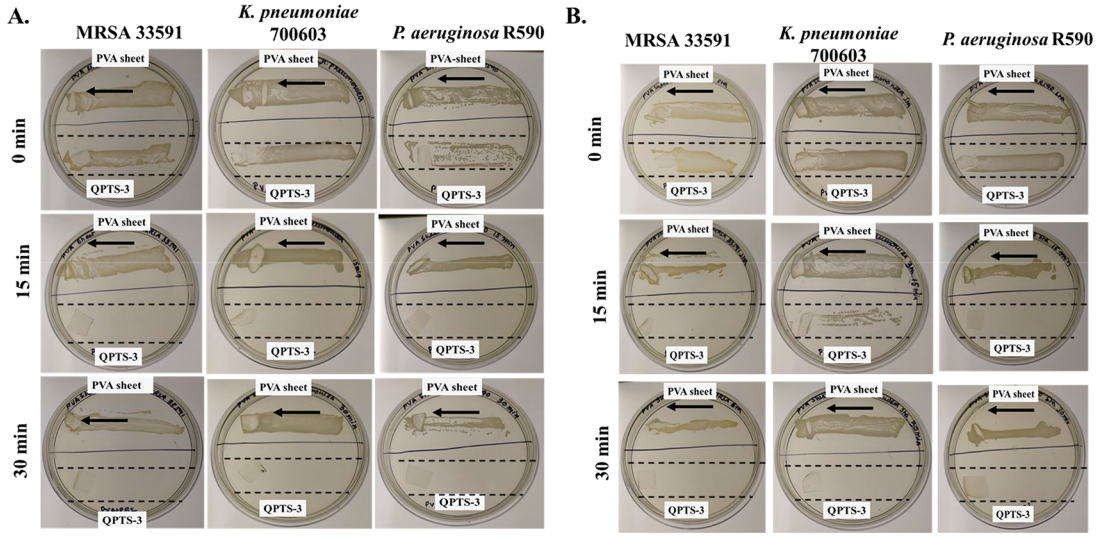

Figure 4. Bactericidal kinetics of the PVA sheet and QPTS-3 against (A) planktonic cells of bacteria and (B) stationary cells of bacteria. The arrow indicates the direction of dragging of the sheet on the agar plate. Dotted lines indicate the path of dragging.

turbidity method, clear media solution without any turbidity was observed in the QPTS-3 treated sample.

This data confirmed that, even after multiple cleaning cycles, the bactericidal efficacy of the QPTS-3 sheet was retained (Figure 2B).

3.3. Antibacterial Activity of a Transparent Sheet (QPTS-3) through the Drag Method. *3.3.1. Antibacterial Activity against Planktonic Bacterial Cells.* Sheets (PVA sheet and QPTS-3) were exposed to ~10^4 CFU cells of Gram-positive bacteria (MRSA ATCC 33591) and Gram-negative bacteria (*E. coli* MTCC 443, *A. baumannii* MTCC 1425, *P. aeruginosa* ATCC 424, *E. coli* R3336, *P. aeruginosa* R590, *K. pneumoniae* ATCC 700603, and *A. baumannii* R674) including various drug-resistant and clinical isolates to verify the bactericidal efficacy (Figure 2C). Bacterial cell-incubated sheets were dragged onto the nutrient agar plates after a 1 h incubation period. No bacterial colony was detected after QPTS-3 treatment, whereas a thick patch of bacterial cells was observed in the case of the PVA sheet treatment (Figure 2C).

3.3.2. Antibacterial Activity against Stationary Bacterial Cells. Killing efficiencies of the sheets (PVA sheet and QPTS-3) were performed against stationary bacteria cells which are difficult to treat with conventional strategies. When the ~10^4 CFU stationary bacteria cells (MRSA ATCC 33591, *E. coli* MTCC 443, *A. baumannii* MTCC 1425, *P. aeruginosa* ATCC 424, *E. coli* R3336, *P. aeruginosa* R590, *K. pneumoniae* ATCC 700603, and *A. baumannii* R674) were incubated with sheets for 1 h, the control sheet (PVA sheet) exhibited a lawn of bacteria. QPTS-3 showed no growth of a bacterial colony, confirming the efficacy of the sheets to inactivate stationary phase bacteria cells (Figure 3). Overall, the QPTS-3 sheet completely killed both planktonic and stationary phase bacteria cells.

3.4. Time-Kill Kinetics of Sheets. *3.4.1. Bactericidal Kinetics.* A rapid killing of the viable bacterial burden is necessary to mitigate the infection-spread through surfaces. Therefore, time kill kinetics of the sheets (PVA sheet and QPTS-3) against bacteria (MRSA ATCC 33591, *K. pneumoniae* ATCC 700603, and *P. aeruginosa* R590) was performed against both planktonic and stationary bacteria cells (~10^4 CFU cells) up to 30 min (Figure 4). At different time points (0, 15, and 30 min), the bacteria-laden sheets were dragged on the agar plates to observe the bacterial growth. At 0 min, the control sheet (PVA sheet) and the QPTS-3 both exhibited the presence of a patch of bacteria against MRSA, *K. pneumoniae*, and *P. aeruginosa* cells, whereas after a 15 min interval, the patch of bacteria was still present in the PVA sheet, but no bacterial growth was detected in the case of QPTS-3, proving its rapid bactericidal nature (Figure 4A).

When the stationary cells were exposed to the sheets (PVA sheet and QPTS-3) for different time points, at 0 min, the control sheet (PVA sheet) and the QPTS-3 both exhibited the presence of a patch of bacteria against MRSA, *K. pneumoniae*, and *P. aeruginosa* cells. After a 15 min interval, the patch of

https://doi.org/10.1021/acsabm.2c00476
ACS Appl. Bio Mater. 2022, 5, 3951−3959

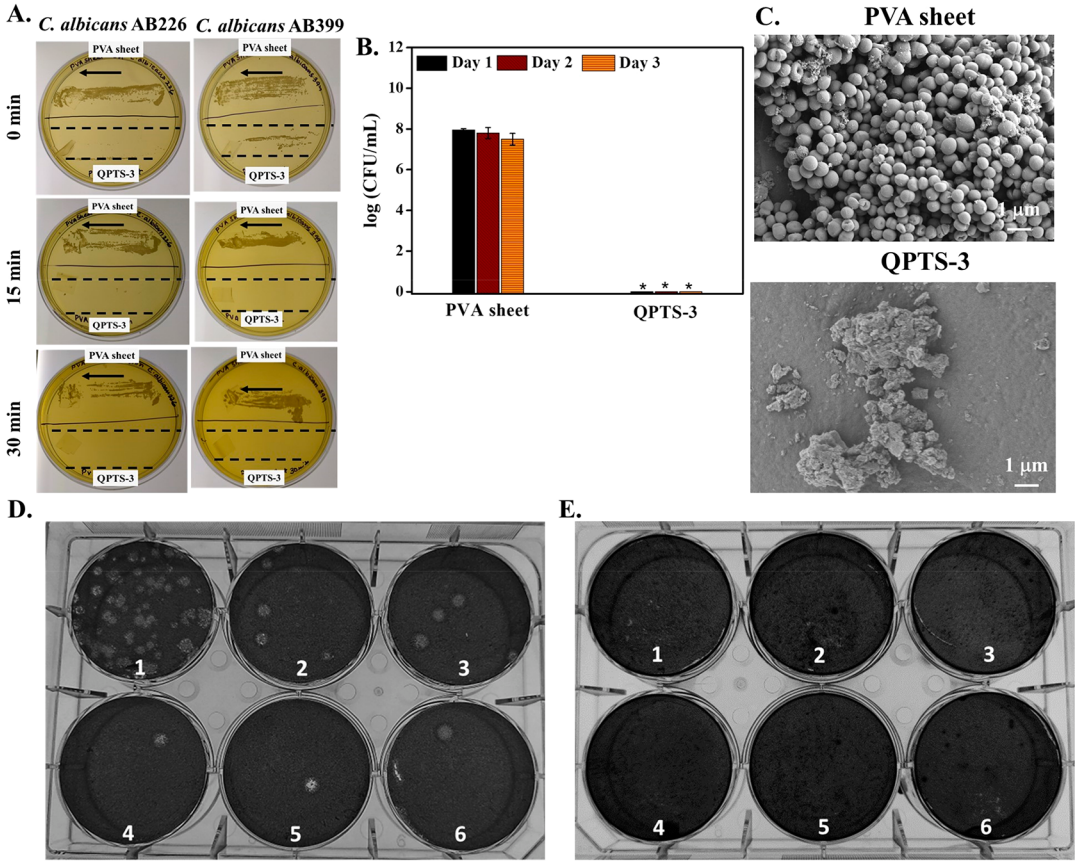

Figure 5. (A) Fungicidal kinetics of the control sheet (PVA sheet) and antimicrobial transparent sheet (QPTS-3) against *C. albicans* strains. (B) Biofilm inhibition efficacy of the PVA sheet and QPTS-3 against MRSA ATCC 33591. (C) Visualization of MRSA biofilm inhibition on the PVA sheet and QPTS-3 through FESEM. Scale bar was 1 μm. The asterisk (∗) indicates a bacterial presence <50 CFU/mL. The anti-influenza activity of polymeric sheets was observed by a plaque assay against the A/NWS/33 strain (H1N1). (D) PVA sheet treatment: 100-fold dilution (well 1) and its 2-fold serial dilution (wells 2−6). (E) QPTS-3 treatment: without further dilution (well 1) and its 2-fold serial dilution (wells 2−6). No plaque forming unit at well 1 indicates that the viral load is <5 PFU/mL. Dotted lines indicate the path of dragging.

bacteria was still present in PVA sheets, but no bacterial growth was detected in the QPTS-3-treated case against MRSA and *P. aeruginosa*. In the case of *K. pneumoniae*, after 15 min of exposure, a slight reduction of the bacterial cells was observed, and there was a complete reduction in the stationary bacterial cells within 15−30 min. QPTS-3 completely reduced the stationary bacterial cells within 15−30 min of exposure (Figure 4B).

3.4.2. Fungicidal Kinetics. A rapid killing of the viable fungal burden is also necessary to mitigate the infection spread. *C. albicans* strains are one of the deadliest human pathogens and can cause multitudes of infections such as chronic skin infection, bloodstream infection, ear infection, lung infection, urinary tract infection, etc.[23−26] Therefore, QPTS-3 was exposed to the fluconazole-resistant fungal strains (*C. albicans* AB226, and *C. albicans* AB399, ∼10^4 CFU cells) for up to 30 min. At 0 min, the control sheet (PVA sheet) exhibited the presence of a patch of fungi against both *C. albicans* strains. QPTS-3 showed a slight reduction on the agar plate (0−2 min) against *C. albicans* AB226 and *C. albicans* AB399. On the contrary, the patch of fungi was still present in the PVA sheet after 15 min of exposure, but no fungal growth was detected in the QPTS-3-treated cases against both *C. albicans* strains (Figure 5A). These results suggested that the antimicrobial sheet can effectively eradicate fungal cells and can stop the surface-associated transmission of microbial infections.

3.5. Inhibition of Biofilm Formation on Sheets. Accumulation of bacteria on abiotic surfaces sometimes leads to biofilm formation which is very difficult to eradicate with traditional regimens.[27] Sheets (PVA sheet and QPTS-3) were immersed in the MRSA cell suspension in biofilm media for different time periods (24, 36, and 72 h), and viable bacterial-counting was performed. Almost 7.5−7.9 log bacterial cells were detected in the biofilm formed on the PVA sheet (Figure 5B). However, no viable bacterial cells were detected in QPTS-3 treated cases, which implied inhibition of bacterial colonization on the cationic PEI derivative embedded transparent sheet.

FESEM imaging was employed to visualize the antibiofilm property of this antimicrobial sheet (QPTS-3). In the case of only the PVA sheet, a large number of round-shaped adhered MRSA cells were imaged through FESEM which confirmed the bacterial colonization on the control sheet. When QPTS-3 treated bacteria were imaged after 72 h, no live bacteria were traced onto the sheet (Figure 5C). The presence of only bacterial debris onto the QPTS-3 sheet also validates that the QPTS-3 sheet inhibited the bacterial growth as well as killed them upon contact. Therefore, this antimicrobial sheet can efficiently stop bacterial accumulation followed by biofilm formation.

3.6. Antiviral Activity of Transparent Sheets. Propagation of various viral infections through fomites or direct

https://doi.org/10.1021/acsabm.2c00476
ACS Appl. Bio Mater. 2022, 5, 3951−3959

human interaction is expected to be inhibited through surface coatings or surface coverings. To evaluate the antiviral activity of these sheets (PVA sheet and QPTS-3), ~8×10^3 PFU viral cells (10 μL of ~8×10^5 PFU/mL) of enveloped influenza H1N1 (A/NWS/33) were exposed to the sheet surfaces. When the control PVA sheet was exposed to the viral cells for 30 min, ~3×10^3 PFU/mL viral cells were detected through a plaque assay (Figure 5D). However, 30 min of incubation of the viral cells onto the QPTS-3 sheet completely reduced (~3.5 log, >99.9%) the viral load, and no plaque forming unit was observed (Figure 5E). This data suggests that the QPTS-3 sheet can efficiently reduce the viral burden which can easily inhibit the viral transmission.

4. CONCLUSION

In conclusion, an easy-to-synthesize polymeric sheet (QPTS-3) was fabricated, which showed an excellent antimicrobial property and was transparent in nature. The sheet rapidly inactivated bacteria and fungi cells including their drug-resistant and clinical isolates. The QPTS-3 sheet also prevented bacterial accumulation onto the surface and inhibited their biofilm formation. After multiple washing cycles, this sheet can be reused, as it retained its antimicrobial activity. A significant reduction of influenza virus upon exposure to this sheet was also observed within a short period of time. In addition, the transparent nature of this sheet can broaden the potential use of this material in commercial and hospital settings.

■ ASSOCIATED CONTENT

Supporting Information

The Supporting Information is available free of charge at https://pubs.acs.org/doi/10.1021/acsabm.2c00476.

Schematic and brief description of the preparation of QPEINH-C_6, thermogravimetric analysis, and DSC data of the sheets (PDF)

■ AUTHOR INFORMATION

Corresponding Author

Jayanta Haldar − *Antimicrobial Research Laboratory, New Chemistry Unit and School of Advanced Materials, Jawaharlal Nehru Centre for Advanced Scientific Research (JNCASR), Bengaluru 560064 Karnataka, India;* orcid.org/0000-0002-8068-1015; Email: jayanta@jncasr.ac.in

Authors

Brinta Bhattacharjee − *Antimicrobial Research Laboratory, New Chemistry Unit, Jawaharlal Nehru Centre for Advanced Scientific Research (JNCASR), Bengaluru 560064 Karnataka, India*

Sudip Mukherjee − *Antimicrobial Research Laboratory, New Chemistry Unit, Jawaharlal Nehru Centre for Advanced Scientific Research (JNCASR), Bengaluru 560064 Karnataka, India*

Riya Mukherjee − *Antimicrobial Research Laboratory, New Chemistry Unit, Jawaharlal Nehru Centre for Advanced Scientific Research (JNCASR), Bengaluru 560064 Karnataka, India*

Complete contact information is available at: https://pubs.acs.org/10.1021/acsabm.2c00476

Notes

The authors declare no competing financial interest.

■ ACKNOWLEDGMENTS

B.B. thanks CSIR for a fellowship. S.M. thanks JNCASR for a fellowship. R.M. thanks IUSSTF (Indo-U.S. Science and Technology Forum).

■ REFERENCES

(1) van Seventer, J. M.; Hochberg, N. S. Principles of Infectious Diseases: Transmission, Diagnosis, Prevention, and Control. In *International encyclopedia of public health*; Elsevier, 2017; pp 22−39.

(2) Hoque, M. N.; Akter, S.; Mishu, I. D.; Islam, M. R.; Rahman, M. S.; Akhter, M.; Islam, I.; Hasan, M. M.; Rahaman, M. M.; Sultana, M.; Islam, T.; Hossain, M. A. Microbial Co-Infections in COVID-19: Associated Microbiota and Underlying Mechanisms of Pathogenesis. *Microb. Pathog* **2021**, *156*, 104941.

(3) Nalbandian, A.; Sehgal, K.; Gupta, A.; Madhavan, M. V.; McGroder, C.; Stevens, J. S.; Cook, J. R.; Nordvig, A. S.; Shalev, D.; Sehrawat, T. S.; Ahluwalia, N.; Bikdeli, B.; Dietz, D.; Der-Nigoghossian, C.; Liyanage-Don, N.; Rosner, G. F.; Bernstein, E. J.; Mohan, S.; Beckley, A. A.; Seres, D. S.; Choueiri, T. K.; Uriel, N.; Ausiello, J. C.; Accili, D.; Freedberg, D. E.; Baldwin, M.; Schwartz, A.; Brodie, D.; Garcia, C. K.; Elkind, M. S. V.; Connors, J. M.; Bilezikian, J. P.; Landry, D. W.; Wan, E. Y. Post-Acute COVID-19 Syndrome. *Nat. Med.* **2021**, *27* (4), 601−615.

(4) Flerlage, T.; Boyd, D. F.; Meliopoulos, V.; Thomas, P. G.; Schultz-Cherry, S. Influenza Virus and SARS-CoV-2: Pathogenesis and Host Responses in the Respiratory Tract. *Nat. Rev. Microbiol* **2021**, *19* (7), 425−441.

(5) Costerton, J. W.; Stewart, P. S.; Greenberg, E. P. Bacterial Biofilms: A Common Cause of Persistent Infections. *Science* **1999**, *284* (5418), 1318−1322.

(6) Campoccia, D.; Montanaro, L.; Arciola, C. R. A Review of the Biomaterials Technologies for Infection-Resistant Surfaces. *Biomaterials* **2013**, *34* (34), 8533−8554.

(7) Blanco-Cabra, N.; Vega-Granados, K.; Moya-Andérico, L.; Vukomanovic, M.; Parra, A.; Alvarez de Cienfuegos, L.; Torrents, E. Novel Oleanolic and Maslinic Acid Derivatives as a Promising Treatment against Bacterial Biofilm in Nosocomial Infections: An in Vitro and in Vivo Study. *ACS Infect. Dis* **2019**, *5* (9), 1581−1589.

(8) Kligman, A.; Dastmalchi, K.; Smith, S.; John, G.; Stark, R. E. Building Blocks of the Protective Suberin Plant Polymer Self-Assemble into Lamellar Structures with Antibacterial Potential. *ACS Omega* **2022**, *7* (5), 3978−3989.

(9) Bhattacharjee, B.; Ghosh, S.; Patra, D.; Haldar, J. Advancements in Release-Active Antimicrobial Biomaterials: A Journey from Release to Relief. *Wiley Interdiscip. Rev. Nanomed. Nanobiotechnol* **2021**, *14* (1), No. e1745.

(10) Ghosh, C.; Sarkar, P.; Issa, R.; Haldar, J. Alternatives to Conventional Antibiotics in the Era of Antimicrobial Resistance. *Trends Microbiol* **2019**, *27* (4), 323−338.

(11) Roy, A.; Basuthakur, P.; Haque, S.; Patra, C. R. Silver-based Nanoparticles for Antibacterial Activity: Recent Development and Mechanistic Approaches. In *Microbial interactions at nanobiotechnology interfaces: molecular mechanisms and applications*; Krishnaraj, R. N., Sani, R. K., Eds.; Wiley, 2021; pp 245−301.

(12) Mukherjee, S.; Barman, S.; Mukherjee, R.; Haldar, J. Amphiphilic Cationic Macromolecules Highly Effective Against Multi-Drug Resistant Gram-Positive Bacteria and Fungi With No Detectable Resistance. *Front. Bioeng.* **2020**, *8*, 55.

(13) Leung, N. H. L. Transmissibility and Transmission of Respiratory Viruses. *Nat. Rev. Microbiol* **2021**, *19* (8), 528−545.

(14) Tellier, R.; Li, Y.; Cowling, B. J.; Tang, J. W. Recognition of Aerosol Transmission of Infectious Agents: A Commentary. *BMC Infect. Dis* **2019**, *19* (1), 101.

(15) Wang, C. C.; Prather, K. A.; Sznitman, J.; Jimenez, J. L.; Lakdawala, S. S.; Tufekci, Z.; Marr, L. C. Airborne Transmission of Respiratory Viruses. *Science* **2021**, *373* (6558), abd9149.
(16) Ghosh, S.; Haldar, J. Cationic Polymer-Based Antibacterial Smart Coatings. In *Advances in smart coatings and thin films for future industrial and biomedical engineering applications*; Elsevier, 2020; pp 557−582.
(17) Ahmed, W.; Zhai, Z.; Gao, C. Adaptive Antibacterial Biomaterial Surfaces and Their Applications. *Mater. Today Bio* **2019**, *2*, 100017.
(18) Bhattacharjee, B.; Jolly, L.; Mukherjee, R.; Haldar, J. An Easy-to-Use Antimicrobial Hydrogel Effectively Kills Bacteria, Fungi, and Influenza Virus. *Biomater. Sci.* **2022**, *10*, 2014−2028.
(19) Ghosh, S.; Mukherjee, R.; Basak, D.; Haldar, J. One-Step Curable, Covalently Immobilized Coating for Clinically Relevant Surfaces That Can. Kill Bacteria, Fungi, and Influenza Virus. *ACS Appl. Mater. Interfaces* **2020**, *12* (25), 27853−27865.
(20) Engelke, L.; Winter, G.; Engert, J. Application of Water-Soluble Polyvinyl Alcohol-Based Film Patches on Laser Microporated Skin Facilitates Intradermal Macromolecule and Nanoparticle Delivery. *Eur. J. Pharm. Biopharm* **2018**, *128*, 119−130.
(21) Abdullah, Z. W.; Dong, Y. Biodegradable and Water Resistant Poly(Vinyl) Alcohol (Pva)/Starch (St)/Glycerol (Gl)/Halloysite Nanotube (HNT) Nanocomposite Films for Sustainable Food Packaging. *Front. Mater.* **2019**, *6*, 58.
(22) Ben Halima, N. Poly(Vinyl Alcohol): Review of Its Promising Applications and Insights into Biodegradation. *RSC Adv.* **2016**, *6* (46), 39823−39832.
(23) Gow, N. A. R.; van de Veerdonk, F. L.; Brown, A. J. P.; Netea, M. G. Candida Albicans Morphogenesis and Host Defence: Discriminating Invasion from Colonization. *Nat. Rev. Microbiol* **2012**, *10* (2), 112−122.
(24) Kullberg, B. J.; Arendrup, M. C. Invasive Candidiasis. *N. Engl. J. Med.* **2015**, *373* (15), 1445−1456.
(25) Carolus, H.; Van Dyck, K.; Van Dijck, P. Candida Albicans and Staphylococcus Species: A Threatening Twosome. *Front. Microbiol* **2019**, *10*, 2162.
(26) Filkins, L. M.; O'Toole, G. A. Cystic Fibrosis Lung Infections: Polymicrobial, Complex, and Hard to Treat. *PLoS Pathog* **2015**, *11* (12), No. e1005258.
(27) Busscher, H. J.; van der Mei, H. C.; Subbiahdoss, G.; Jutte, P. C.; van den Dungen, J. J. A. M.; Zaat, S. A. J.; Schultz, M. J.; Grainger, D. W. Biomaterial-Associated Infection: Locating the Finish Line in the Race for the Surface. *Sci. Transl. Med.* **2012**, *4* (153), 153rv10.

https://doi.org/10.1021/acsabm.2c00476
ACS Appl. Bio Mater. 2022, 5, 3951−3959